



# Prediction of compressive strength of concretes containing micro silica subject to carbonation using neural network

A.O Akbari moghaddam <sup>a</sup>, A. Delnavaz <sup>b, ✉</sup>, S.A.H Hashemi <sup>b</sup>, S.H Ghasemi <sup>c</sup>,

<sup>a</sup> Department of Civil Engineering, Qazvin Branch, Islamic Azad University, Qazvin, Iran

<sup>b</sup> Department of civil engineering, Qazvin branch, Islamic Azad University, Qazvin, Iran

<sup>c</sup> Department of civil and environmental engineering, Rowan University, Glassboro, NJ08028, USA

Received 10 January 2023; Revised 01 February 2023; Accepted 10 March 2023

✉ A.Delnavaz@qiau.ac.ir

## Abstract

Concrete materials are exposed to special weather conditions, corrosion and significant damage. For this purpose, the effect of 28-day compressive strength changes on the samples studied in this study was investigated by considering the simultaneous effect of chloride ion penetration and carbonation phenomenon. For this reason, in the first case, the samples are exposed to carbon dioxide once and then to chloride ions. In the latter case, only samples under the influence of chloride infiltration are examined. To make the samples, which include 9 mixing designs, three water-to-cement ratios of 0.35, 0.4 and 0.5 and three percent of 0%, 7% and 10% silica fume have been used. Finally, an optimal model is introduced to predict the compressive strength of concrete containing micro silica exposed to carbonation using artificial neural network. Also, a relation for estimating compressive strength based on the ratio of water to cement and the amount of silica is presented.

**Keywords:** Compressive Strength, Concrete, Silica Fume, Carbonation, Artificial Neural Network

## 1. Introduction

Despite the high durability of concrete compared to steel, but concrete materials in severe corrosive environments such as coasts and ports and islands of the Persian Gulf and the Sea of Oman are severely damaged and therefore their useful life is greatly reduced. Reinforcement corrosion in reinforced concrete is due to the penetration of chloride ions and carbonation of concrete. Reinforcement corrosion in concrete is one of the major damages to reinforced concrete structures. One of the unfavorable areas for the destruction of reinforced concrete structures is the coasts and islands of the Persian Gulf. On the other hand, due to the industrialization of the region, changes in the concentration of pollutants, including CO<sub>2</sub> gas in the region can be predicted. Infiltration of gases in the environment and the formation of acids lead to changes in the pH of concrete. Among the effective gases are CO<sub>2</sub> in the air and SO<sub>3</sub> in rainwater. The role of carbon dioxide in this process is considerable. With the penetration of carbon dioxide in concrete, the phenomenon of carbonation occurs. In the carbonation phenomenon, a chemical reaction takes place between the carbon dioxide that has penetrated into the concrete and the alkaline products resulting from the hydration of the cement. This reaction leads to the formation of soluble calcium salts [1-2]. So far, many researchers have studied the properties of silica [3-4]. Page and Vennesland investigated the possibility of increasing the solubility of Friedel salt in microsilica-containing cements. In their study, this group made concrete samples with 10%, 20%

and 30% microsilica instead of cement and observed changes in pore alkalinity and chloride entrapment [5]. Swami and Suryavanshi investigated the effect of carbonation on the stability of Friedel salt. Some of different concrete slabs were constructed with water to cement ratios (w / b) and the use of mineral additives such as microsilica, steel furnace slag, and fly ash. The slabs were subjected to wet and dry cycles. The results showed that the solubility of Friedel salt increased in carbonate regions [6]. Ishida and Maekawa Using thermodynamic equations and mass transfer governing concrete, proposed a finite element model to predict the useful life of reinforced concrete structures. This computational model was presented in software called DuCOM, which can model failure phenomena in concrete and thermal analysis [7-9]. Lin and Liang investigated the simultaneous effect of chemicals on reinforced concrete structures using one-dimensional diffusion equations. They proposed an analytical solution of the diffusion equation using the Laplace transform method and the Convolution theorem. Also, the simultaneous effect of Cl<sup>-</sup> and CO<sub>2</sub> as well as Cl<sup>-</sup> and SO<sub>4</sub><sup>2-</sup> as well as CO<sub>2</sub> and SO<sub>4</sub><sup>2-</sup> was included in the equations. To consider the simultaneous effect of the above compounds, this group used a delay coefficient R in their equations to investigate the effect of each ion on the other [10]. Razzaqpour et al. presented a numerical model to consider the simultaneous effect of temperature transfer, humidity, chloride penetration, and carbonation phenomenon in concrete. The proposed model includes a numerical solution of two-dimensional equations governing infiltration. In this study, the finite element

method was used to solve the equations. The effect of carbonation on the change of concrete pore structure and its interaction with moisture and chloride transfer is considered in this model. The effect of carbonation on chloride release is not included in this group. The model of this group is presented in software called CONDOUR [11]. Putatsannan and Soma presented a nonlinear numerical model for the simultaneous penetration of chloride and carbonation into concrete. The model of this group was very similar to the model presented by Razaqpour. The difference was that this group used the finite difference method to solve the equations. Heat, relative humidity, chloride penetration, and carbonation are the phenomena that were studied in this group as finite difference models. The effect of simultaneous diffusion of chloride and carbonation in two models of homogeneous and heterogeneous concrete has been investigated [12]. Song et al. presented a numerical model to predict the useful life of reinforced concrete structures under the simultaneous influence of chloride and carbonation. The model presented by this group is somewhat similar to Ishida, which includes models of thermal hydration of concrete components, model of microstructure formation, mass transfer model, chloride penetration, and carbonation and corrosion model of steel. In the model presented by this group, the finite element method was used to solve the equations governing the infiltration phenomenon. This model can also model the failure due to the simultaneous effects of moisture penetration, chloride and structural changes of concrete under the effect of carbonation. The model of this group considers the effect of carbonation on the release of chloride through experimental equations. The results of the proposed model for chloride infiltration were validated with the results of sampling of a river bridge [13]. Ameli et al. deal with the development of an environmentally sustainable roller compacted concrete. The variables used were; high volume fly ash (HVFA) at 50%, 60%, and 70% replacement by volume; crumb rubber at 10%, 20%, and 30% replacement by volume of fine aggregate; nano silica at 0%, 1%, and 2% addition by weight of cementitious materials. The addition of nano silica increases the Vebe time, fresh density, compressive strength, flexural strength, splitting and tensile strength of HVFA RCC [14]. Since the compressive strength of concrete specimens is a very important parameter in the evaluation of concrete specimens, many researchers have used soft calculations and its tools to provide models for predicting this parameter. One of the advantages of these methods is the prediction of compressive strength at the desired age with different ratios of the mixing plan in just a few hours; In addition to saving materials, it leads to the

correct use of time, which is an important parameter in carrying out projects. One of the most widely used methods of prediction is the use of artificial neural network method. So far, many researchers have predicted different properties of concrete by designing different models of neural networks [15-21]. One of the most important properties of hardened concrete is the compressive strength of concrete. Many different properties of concrete such as specific gravity, permeability, partial durability, abrasion resistance, sulfate resistance, tensile strength and some other properties are a function of compressive strength [22-24]. In this research, based on laboratory methods, concrete samples are made in two states of fully carbonated and ordinary non-carbonated concrete exposed to chloride ions, and then the compressive strength test is performed on the mentioned samples. The following is a neural network model for predicting compressive strength for concrete specimens studied in this study

not hinder you, in authoring your paper. It should follow you in how you want to write your paper, not force you to fill in bits and pieces of text. It should allow you to type any text, copy from previous versions, or load an already existing plain text to be formatted. You will therefore find no dialog boxes or fill-in screens. You will not need to remember shortcut keys, to use lists of styles, bother about alignment, indents, fonts and point sizes. Just a mouse-click at one of the menu options will give you the style that you want.

The objective of this template is to enable you in an easy way to style your article attractively in a style similar to that of *QJIE*. It should be emphasized, however, that the final appearance of your paper in print and in electronic media will very likely *vary to greater or lesser extent* from the presentation achieved in this Word® document.

## 2. Methods

### 2.1. Materials

ASTM Type I-425 Portland cement with a specific gravity of 3.15 and silica-fume with a specific gravity of 2.90 was used. Nine mix designs, each with a cementitious material content of 400 kg/m<sup>3</sup>, were used. The W/CM ratios were 0.35, 0.4 and 0.5. The silica fume replacements for cement on a dry mass basis were 0, 7% and 10%. Table 1 shows the properties of various mixture designs in this investigation.

Coarse aggregate with a size range of 6,20 mm was used. The fine aggregate was river sand with a maximum size of 4 mm and fineness modulus of 3.

Table 1: Physical and chemical properties of ordinary Portland cement and SF

		Chemical composition: %								Specific gravity	Blaine: cm <sup>2</sup> /g
		SiO <sub>2</sub>	Al <sub>2</sub> O <sub>3</sub>	Fe <sub>2</sub> O <sub>3</sub>	CaO	MgO	Na <sub>2</sub> O	K <sub>2</sub> O	Ig.loss		
Ordinary Portland cement		21.5	3.68	2.76	61.5	4.8	0.12	0.95	1.35	3.15	3
SF		96	0.6	0.6	0.3	0.5	0.1	0.2	1.7	2.9	3.83

### 2.2. Mixing and preparation of specimens

Nine mix designs, each with a cementitious material content of 400 kg/m<sup>3</sup>, were used. The water-to-cement (w/c) ratios were 0.35, 0.4 and 0.5. The SF replacements for cement on a dry mass basis were 0, 7% and 10%. Table 2 shows the properties of various mixture designs in this investigation. In this table, C represents the amount of cement and Csf indicates the amount of microsilica. Specimens were cast in moulds of 100 \* 100 \* 100 mm cubes, and 100 \* 200 mm cylinders. The specimens were exposed to chloride in three different conditions for more than 270 days at 38°C. The superplasticizer used in making the samples was also selected from the neutral type without chloride ions. The

construction of the samples was done according to the ABA regulations. In making samples, a slump between 5 and 7 cm is considered as a slump. The samples were processed in containers containing saturated lime water solution at a temperature of 21 ± 2 °C.

It should be noted that due to the fact that the penetration depth in the samples was about 2.5 cm in the maximum case, so the selection of the sample size had no effect on the results. Also, according to the dimensions of the experimental samples, the maximum aggregate dimension was limited to 2.5 cm. However, according to previous studies, the maximum aggregate has been little considered in the diffusion models and its effect on the chloride ion diffusion coefficient is not very significant.

Table 2: Mix proportions of concretes

Mix ID	W/(c+csf)	Csf/(c+csf)	Water kg/m <sup>3</sup>	Cement kg/m <sup>3</sup>	Gravel kg/m <sup>3</sup>	Sand kg/m <sup>3</sup>	SF kg/m <sup>3</sup>
M-35-0	0.35	0	140	400	1050	800	0
M-35-7	0.35	7%	140	372	1050	800	28
M-35-10	0.35	10%	140	360	1050	800	40
M-40-0	0.4	0	160	400	1050	800	0
M-40-7	0.4	7%	160	372	1050	800	28
M-40-10	0.4	10%	160	360	1050	800	40
M-50-0	0.5	0	200	400	1050	800	0
M-50-7	0.5	7%	200	372	1050	800	28
M-50-10	0.5	10%	200	360	1050	800	40

### 2.3. Carbonate the samples

Due to the fact that the purpose of this study is to investigate the effect of carbonation on changing the properties of concrete, so the samples were tested in both carbonate and non-carbonate states. In order to carbonate the concrete, the samples, after 28 days of curing, a number of samples were subjected to CO<sub>2</sub> gas for 1 month to perform the carbonation process in the carbonation machine at 60% humidity. Control samples were also placed in the tank to control the carbonation of the samples. The amount of incoming gas was determined to occupy at least half of the space inside the tank with carbon dioxide gas. For this purpose, the amount of

exhaust gas was determined according to the exhaust gas flow rate (observed from the regulator degree) and time measurement. However, due to the possibility of gas leakage, gas injection was performed several times. Phenolphthalein solution was used to control the carbonation depth of the control samples. Carbonated samples along with control samples were exposed to chloride ion for 270 days in three submerged environmental conditions, tides and above water level (atmosphere). The concentration of chloride ion in the medium was considered to be 30 gr / lit.

### 3. Results and Discussion

#### 3.1. Compressive strength of samples

Compressive strength test was performed on 10 cm cubic specimens at 28 days according to ASTM C39 standard.

Table 3 shows the average results on the three samples for each mixing scheme.

Table 3: Compressive strength test results of samples

Mix ID	Non-carbonated concrete		carbonated concrete	
	Age(days)		Age(days)	
	28	90	28	90
M-35-0	453	462	436	456
M-35-7	525	559	537	552
M-35-10	595	629	593	632
M-40-0	400	397	394	408
M-40-7	498	536	490	524
M-40-10	528	569	532	555
M-50-0	372	382	366	379
M-50-7	448	453	443	460
M-50-10	496	518	490	513

Figure 1 show the strength of carbonated and non-carbonated samples based on the type of mixing design and the age of the samples. As can be seen, the resistance changes in the samples do not have a specific trend based on whether the samples are carbonate or not, and practically carbonation does not cause a significant change in the strength of the samples. The reason for this can be considered in the low carbonation depth compared to the sample dimensions. In other words, despite the fact that it is expected that the strength of this layer will increase with surface carbonation, but because the strength of the cubic sample is more affected by the middle layers of concrete, the effect of carbonation on changing the strength is not obvious.

#### 3.2. Artificial neural networks

One of the most widely used models in soft computing is the neural network, which is inspired by the human brain and includes weighted connections between artificial neurons. In general, in neural networks, there are three types of neural layers: the input layer, which is responsible for receiving raw information. Hidden layers where the performance of these layers is determined by the inputs and the weight of the connection between them and the hidden layers. The output layer also depends on the activity of the hidden unit and the weight of the connection between the hidden unit and the output. The difference between the output of the neural network and the desired output is defined as the error function. The

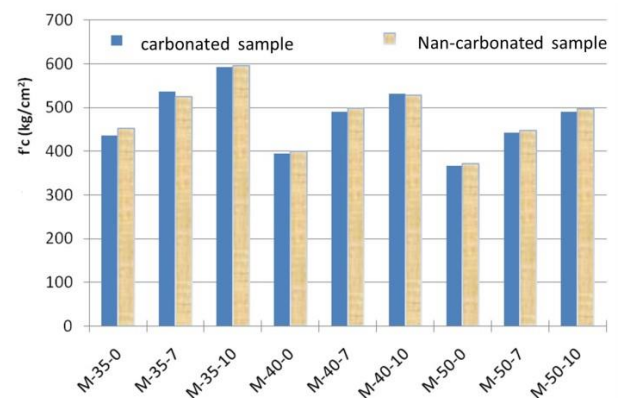


Fig.1. Results of compressive strength testing at 28 days age

error is then reversed and the weights and biases are corrected to reduce the error. This process, known as the learning step, is repeated until the most accurate determination of the outputs. Validation was also performed indirectly during learning to show the pre-fitting of a neural network. The stopping point of the learning process is when the validation error starts to increase. The last step in modeling an artificial neural network is the experimental step, which is performed only to determine the efficiency of the trained network [25]. Figure 2 shows a schematic representation of a computational neuron and its components.

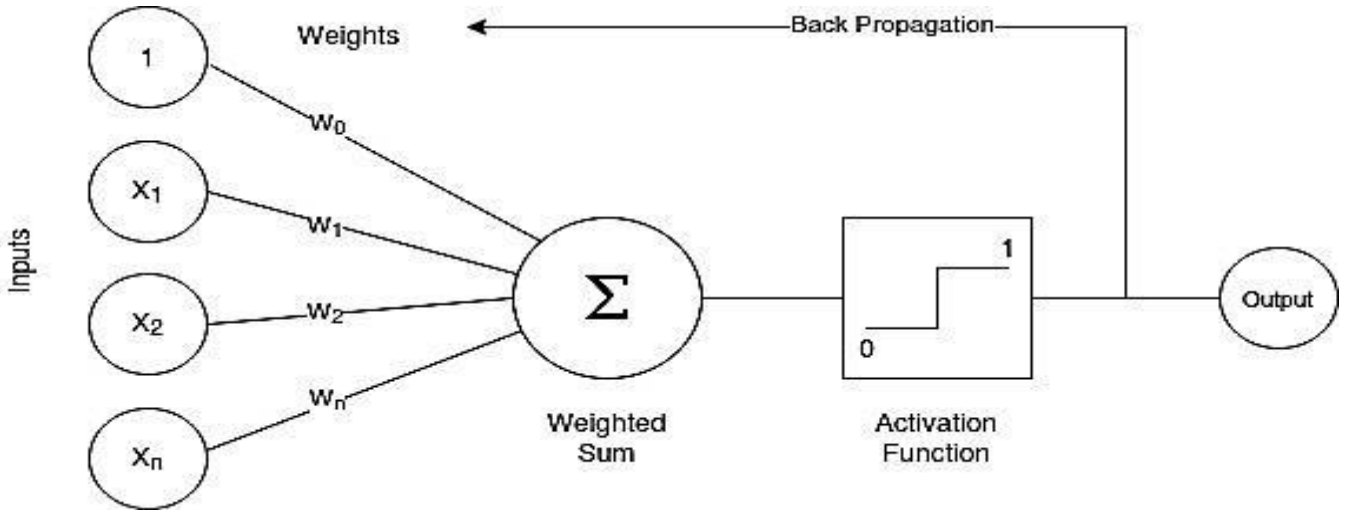


Fig. 1. Single processing element of ANNs

### 3.3. Architecture of neural network model

The software used to build the model of artificial neural networks is MATLAB. This software is a technical language with strong performance in computing that has undergone many changes and improvements over the years and according to the needs of users, including the addition of a neural network toolbox to it. A neural network model was developed to predict compressive strength. In this model, the number of hidden layers as well as the number of neurons in each layer was determined to minimize network error. Network inputs, water to cement ratio, silica content and 28 and 90 days compressive strength were selected as the output. To evaluate the performance and accuracy of the network, two statistical criteria of mean square error (MSE) and correlation coefficient (R) have been used. The relationship between these two criteria is given in Equations (1) and (2). In these relations  $y_i$  are the predicted data,  $x_i$  the measured data,  $\bar{Y}$  the average of the predicted data and  $\bar{X}$  the average of the measured data.

$$1) \quad MSE = \frac{1}{n} \sum_{i=1}^n (x_i - y_i)^2$$

$$2) \quad R = \frac{\sum_{i=1}^n (x_i - \bar{X})(y_i - \bar{Y})}{\sqrt{\sum_{i=1}^n (x_i - \bar{X})^2 \sum_{i=1}^n (y_i - \bar{Y})^2}}$$

To determine the best network model, different models with the number of layers and neurons as well as different training functions in each layer were used. Table 4 shows examples of these models for the carbonate state. One of the problems with neural networks is the need for a lot of data to compare models. In the present model, due to lack of data, it is difficult to compare models. Because the output error of the models in all models was a small number. Also, due to lack of data, it was not possible to delete some of them in order to control the network. For this reason, the following algorithm was used to compare the proposed models:

A. In the first stage, 5 samples of input and output results were used as data for network training so that the network could be trained with the help of this data. After training, the ninth data network was given to the networks used and the network output was compared with the value obtained from the laboratory results and the amount of difference between the test result and the network output was recorded.

B- In the second stage, the process of the first stage was repeated. The difference is that at this stage another mixing scheme result was used to control the network.

C- Steps A and B were used for all mixing designs and in all proposed networks. Finally, the total error of different networks was calculated for 9 times of network training and control, and the network with the lowest error rate was selected as the optimal network.

Table 4. Results of training steps of ANN

ANN model structure	Transfer function	Training		MSE
		Max Error	$R^2$	
2-2-2-1	G-S-S	0.028	0.99	0.12
2-3-2-1	S-S-HT	0.03	0.99	0.15
2-3-2-1	S-HT-G	0.0399	0.99	0.07
2-3-2-1	HT-HT-S	0.0346	0.99	0.08
2-3-2-1	G-HT-S	0.03	0.99	0.14
2-4-3-1	G-HT-S	0.03	0.99	0.10
2-4-3-1	HS-G-S	0.03	0.99	0.11
2-4-3-1	HT-S-G	0.03	0.99	0.19
2-5-3-1	G-G-S	0.03	0.99	0.17
2-5-3-1	G-S-S	0.03	0.99	0.12
2-5-3-1	HS-G-S	0.03	0.99	0.11
2-6-7-1	HS-G-S	0.028	0.99	0.13
2-6-7-1	S-HT-G	0.03	0.99	0.18
2-6-7-1	S-S-G	0.03	0.99	0.14
2-6-7-1	HT-HT-S	0.03	0.99	0.11

S: Sigmoid, G: Gaussian, HT: Hyperbolic Tangent, HS: Hyperbolic Secant

Based on the mentioned steps and also Table 4, the network with three hidden layers and two neurons in each layer, with sigmoid functions in the first layer, hyperbolic

tangent function in the second layer and Gaussian function in the output layer produces the best results. The best network model is shown in Figure 3.

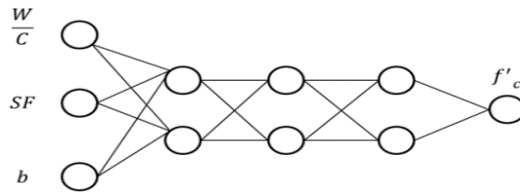


Fig. 3. optimal network model in determining compressive strength

### 3.4. Linear fit model

The following function (Equations (3)) was used to determine the compressive strength. Considering that the

input parameters, water to cement ratio ( $w / c$ ) and SF silica content were considered, the maximum power of the proposed function was selected twice.

$$\begin{aligned}
 3) \quad f'_c = & 1552 - 4960 \left(\frac{W}{c}\right) - 122.384SF + 588.71 \left(\frac{W}{c}\right)SF - 680.635 \left(\frac{W}{c}\right)^2 SF - 156429 \left(\frac{W}{c}\right)SF^2 \\
 & + 18.015 \left(\frac{W}{c}\right)^2 SF^2 + 5200 \left(\frac{W}{c}\right)^2 + 3.394SF^2
 \end{aligned}$$

#### 4. Conclusion

In the present paper, compressive strength in concretes containing silica fume under the influence of carbonation was investigated in a laboratory and a prediction model using a neural network. The procedure was performed in such a way that concrete samples were first carbonated and then compressive strength was performed in carbonate and non-carbonate samples. In total, the following results were obtained from experiments and modeling:

- 1- There are no specific changes in the compressive strength of the samples based on whether the samples are carbonated or not. One of the reasons for this is the low depth of carbonation compared to the dimensions of the sample. Although it is expected that the strength of this layer will increase with surface carbonation, but because the strength of the cubic sample is more affected by the middle layers of concrete, the effect of carbonation on the change in strength is not obvious.
- 2- By using the neural network model proposed in this research, a quadratic function with concrete mix proportion (w/c and SF contents) was developed to predict the effect of carbonation on compressive strength I variations. The model could be useful in prediction of compressive strength in carbonated concrete.

#### References

- [1] Jung, S., Y. Choi, and B. Lee. Influence of carbonation on the chloride diffusion in concrete. SB07 Seoul: Proceedings of the International Conference on Sustainable Building Asia, Seoul, Korea. 2007. <https://doi.org/10.4334/JKCI.2003.15.6.829>.
- [2] Conciatori D, Laferrrière F, Brühwiler E. Comprehensive modeling of chloride ion and water ingress into concrete considering thermal and carbonation state for real climate. *Cement and Concrete Research*. 2010 . 40(1). Pp 109-118. <https://doi.org/10.1016/j.cemconres.2009.08.007>.
- [3] Rassokhin, A.S., Ponomarev, A.N., Figovsky, O.L. Silica fumes of different types for high-performance fine-grained concrete. *Magazine of Civil Engineering*. 2018. No. 78(2). Pp. 151–160. doi: 10.18720/MCE.78.12.
- [4] Abdelgader, H.S., Fediuk, R.S., Kurpinska, M., Khatib, J., Murali, G., Baranov, A.V., Timokhin, R.A. Mechanical properties of two-stage concrete modified by silica fume. *Magazine of Civil Engineering*. 2019. 89(5). Pp. 26–38. DOI: 10.18720/MCE.89.3.
- [5] Page, C.C., Vennesland, O. Effect of Carbonation on Chloride Binding, *Materials and Constructions*. 1983. 16(19).
- [6] Suryavanshi, A. K., and R. Narayan Swamy. Stability of Friedel's salt in carbonated concrete structural elements. *cement and Concrete Research*. 26(5) 1996. Pp 729-741. [https://doi.org/10.1016/S0008-8846\(96\)85010-1](https://doi.org/10.1016/S0008-8846(96)85010-1).
- [7] Maekawa, K., & Ishida, T. Service Life Evaluation of Reinforced Concrete Under Coupled Forces and Environmental Actions. *Proceedings of the JCI*. 2002.20(2). Pp 691-696.
- [8] Maekawa, K., & Ishida, T. Multi-Scale Modeling of Concrete Performance Integrated Material and Structural Mechanics. *Journal of Advanced Concrete Technology*. 2003. 1(2). Pp 91-126.<https://doi.org/10.3151/jact.1.91>.
- [9] Ishida, T., Maekawa, K., & Soltani, M., Theoretical Identified Strong Coupling of Carbonation Rate and Thermodynamic Moisture States in Microspores of Concrete. *Journal of Advanced Concrete Technology*.2004. 2(2). Pp 213-222. <https://doi.org/10.3151/jact.2.213>.
- [10] Liang, M. T., & Lin, S. M. Modeling of Transport of Multiple Chemicals in Concrete Structures: Synergetic Effect Study. *Cement and Concrete Research*. 2003. 33(12). Pp 1917-1924. [https://doi.org/10.1016/S0008-8846\(03\)00081-4](https://doi.org/10.1016/S0008-8846(03)00081-4).
- [11] Isgor, O. B., & Razaqpur, A. G Advanced Modeling of Concrete Deterioration due to Reinforcement Corrosion. *Canadian Journal of Civil Engineering*.2006. 33(6). Pp 707-718. <https://doi.org/10.1139/106-007>.
- [12] Puatatsananon, W., and V. E. Saouma Nonlinear Coupling of Carbonation and Chloride Diffusion in Concrete. *Journal of Materials in Civil Engineering*. 2005. 17(3). Pp 264-275. [https://doi.org/10.1061/\(ASCE\)0899-1561\(2005\)17:3\(264\)](https://doi.org/10.1061/(ASCE)0899-1561(2005)17:3(264)).
- [13] Song, H. W., Pack, S. W., Lee, C. H., & Kwon, S. J. service Life Prediction of Concrete Structures Under Marine Environment Considering Coupled Deterioration. *Restoration of buildings and monuments= Bauinstandsetzen und Baudenkmalpflege*. 2006. 12(4). Pp 265-284.
- [14] Ameli, A. R., Parvaresh Karan, E., & Hashemi, S. A. H. Mechanical Properties and Performance of Roller Compacted Concrete (RCC) Containing High Volume of Fly Ash, Crumb Rubber and Nano Silica using Response Surface Method. *Journal of Transportation Research*. 2018.15(3). Pp 381-395.
- [15] Yeh, I. C. Design of High-performance concrete mixture using neural networks and nonlinear programming. *J. Comput. Civil Eng*. 1999. 13(1). Pp 36-42. [https://doi.org/10.1061/\(ASCE\)0887-3801\(1999\)13:1\(36\)](https://doi.org/10.1061/(ASCE)0887-3801(1999)13:1(36)).
- [16] Yeh, I. C.Exploring concrete slump model using artificial neural networks. *J Comput. Civil Eng*. 2006. 20(3). Pp 217-221. [https://doi.org/10.1061/\(ASCE\)0887-3801\(2006\)20:3\(217\)](https://doi.org/10.1061/(ASCE)0887-3801(2006)20:3(217)).
- [17] Sebastiá, M., Olmo, I. F., & Irabien, A. Neural network prediction of unconfined compressive strength of coal fly ash–cement mixtures. *Cement and Concrete Research*. 2003. 33(8). Pp 1137-1146. [https://doi.org/10.1016/S0008-8846\(03\)00019-X](https://doi.org/10.1016/S0008-8846(03)00019-X).
- [18] Topcu, I. B., & Saridemir, M. Prediction of compressive strength of concrete containing fly ash using artificial neural networks and fuzzy logic. *Computational Materials Science*. 2008. 41(3). Pp

- 305-311.  
<https://doi.org/10.1016/j.commatsci.2007.04.009>.
- [19] Kasperkiewicz, J., Racz, J., & Dubrawski, A. HPC strength prediction using artificial neural network. *Journal of Computing in Civil Engineering*. 1995. 9(4). Pp 279-284.  
[https://doi.org/10.1061/\(ASCE\)0887-3801\(1995\)9:4\(279\)](https://doi.org/10.1061/(ASCE)0887-3801(1995)9:4(279)).
- [20] Peng, J., Li, Z., & Ma, B. Neural network analysis of chloride diffusion in concrete. *Journal of Materials in Civil Engineering*. 2002. 14(4). Pp 327-333.  
[https://doi.org/10.1061/\(ASCE\)0899-1561\(2002\)14:4\(327\)](https://doi.org/10.1061/(ASCE)0899-1561(2002)14:4(327)).
- [21] Ji, T., Lin, T., & Lin, X. A concrete mix proportion design algorithm based on artificial neural networks. *Cement and Concrete Research*. 2006. 36(7). Pp 1399-1408.  
<https://doi.org/10.1016/j.cemconres.2006.01.009>.
- [22] Zarandi, M. F., Türksen, I. B., Sobhani, J., & Ramezani-pour, A. A. Fuzzy polynomial neural networks for approximation of the compressive strength of concrete. *Applied Soft Computing*. 2008. 8(1). Pp 488-498.  
<https://doi.org/10.1016/j.asoc.2007.02.010>.
- [23] Abd Elaty, M. A. A. Compressive strength prediction of Portland cement concrete with age using a new model. *HBRC journal*. 2014. 10(2). Pp 145-155.  
<https://doi.org/10.1016/j.hbrcj.2013.09.005>.
- [24] 24. - Neville, A.M., Brooks, J.J. *Concrete Technology. The Second Edition*. Pennsylvania: Trans-Atlantic Publications, 2010. 354p.
- [25] Naderpour, H., Kheyroddin, A., & Amiri, G. G. Prediction of FRP-confined compressive strength of concrete using artificial neural networks. *Composite Structures*. 2010. 92(12). Pp 2817-2829.  
<https://doi.org/10.1016/j.compstruct.2010.04.00>